A Balanced Hybrid Active-Passive Actuation Approach for High-Performance Haptics

Chembian Parthiban, Patrick Dills, It Fufuengsin, Nick Colonnese, Priyanshu Agarwal and Michael Zinn, *Member, IEEE*

***Abstract*— Hybrid actuation approaches for haptic interfaces generally suffer from asymmetry in rendering and torque capabilities. This paper describes the design of a high-performance balanced hybrid haptic device, which addresses the asymmetry by combining a high-power, low-impedance active compliant actuation (series-elastic actuator) with energy absorbing high-force passive actuation in parallel with a fast, low-power secondary active actuation. We describe the actuation, design and control approaches and experimentally validate the approach with a one degree-of-freedom testbed. The performance is compared with active only approach and results show significant improvements in stability and rendering range of the device.**

I. Introduction

Performance of an impedance-based haptic device is measured by the stable rendering range and device transparency, i.e. its ability to stably and accurately render stiff surfaces and have a low output impedance. Both active and passive actuators have been commonly used to build haptic displays and they serve different purposes.

Active actuators, such as electric motors, can provide high active forces, fast response times and are symmetrical in rendering i.e. they can both restore and dissipate energy. Performance is limited by stability, which is affected by the physical characteristics of the device and the computer interface. Several researchers have studied the effect of compliance, backlash, friction, sampling, encoder quantization, and delay on performance [1-4]. Colgate showed that the rendering range could be improved by adding physical damping to the system [5]. This, coupled with low torque density in active actuators, has led to the use of passive actuators in haptic displays.

Passive actuators have a high torque density, are inherently stable and safe. Since they dissipate energy, they can be used to increase the physical damping of the system and ensure passivity for stable operations [6]. They can render high passive forces as opposed to electrical motors that may require large gear reductions to achieve the same force levels. However, passive actuators are limited in the range of haptic perceptions they can render. They also have relatively slow response times when compared to electric motors, which affects device rendering accuracy and transparency. The slow response time and uncertainty regarding the precise output of the passive actuator can result in a mismatch in the active and passive torques, particularly problematic during periods the desired rendering torque frequently oscillates between large active and passive torque, such as would be the case when interacting with a stiff virtual wall. This is commonly known as the *sticky-effect* [7]. In addition, passive actuators typically have residual torques present when powered off which can affect the device's transparency.

More recently, the use of hybrid actuation – the coordinated use of controlled passive actuators in parallel with active actuators – has been motivated by its demonstrated advantages including high passive force capacity, low external power requirements, low output impedance when deactivated, improved control robustness, and improved passive force rendering. Interest in hybrid actuation has increased as the advantages of passive actuation have been recognized. Specific hybrid actuation configurations that have been investigated include the use of magnetorheological (MR) brakes in parallel with electric actuators [8, 9], dual MR brakes coupled through an overrunning clutch (to reduce the negative effects of the MR brake's nonlinear characteristics) [7], use of a particle brake in series with an elastic spring and an electric actuator [10] and similar configurations using alternative passive actuators such as eddy-current dampers [11]. While improvements in performance and control robustness have been demonstrated using these approaches, they suffer from one or more significant issues which limit their application, including slow response speed and nonlinear hysteresis associated with the passive actuator [12], and a large mismatch between the active and passive actuators, where the passive torque and (dissipative) power capacity can be an order of magnitude larger than the active capacity [7]. In order to address this inherent asymmetry in the rendering capabilities of the active and passive actuator torques in the current hybrid designs, we propose a balanced active-passive actuation approach.

II. Balanced Actuation Approach

The proposed balanced active and passive actuation approach combines a high-power, low-impedance active compliant actuation (series-elastic actuator) with energy absorbing high-force passive actuation in parallel with a fast, low-power secondary active actuation. In general, the inclusion of passive actuation provides high stiffness passive rendering capabilities, aids in control stabilization and helps to minimize power consumption, while the inclusion of the active compliant actuation provides high-force active rendering capabilities and low output impedance. The combined active-passive hybrid system will provide equivalent passive and active force and power output. The fast secondary actuator

Chembian Parthiban, Patrick Dills, It Fufuengsin and Michael Zinn are with the Department of Mechanical Engineering at the University of Wisconsin-Madison. (e-mail: parthiban|pdills|fufuengsin|mzinn@wisc.edu).

Nick Colonnese and Priyanshu Agarwal are with Facebook Reality Labs.

addresses the slow response speeds of both the passive and the active compliant actuation. The proposed combination of active and passive actuation can help realize the advantages of both and aid in overcoming some of the drawbacks associated with each. The passive actuator can extend the rendering range, as shown in [13], while feedback of passive torque error to the active actuation can reduce the sticky-effect and non-linear hysteresis associated with passive actuation techniques.

Figure 1 shows the parallel topology of the proposed actuation approach. The low-impedance nature of the actuators in their respective operating frequency ranges allows the torques to add non-destructively [14] which make the parallel topology possible. This is considered in the design approach where the low-impedance is achieved using a series elastic actuator for the large force active actuation and a low inertia servomotor and brake for the fast secondary active and passive actuators, respectively.

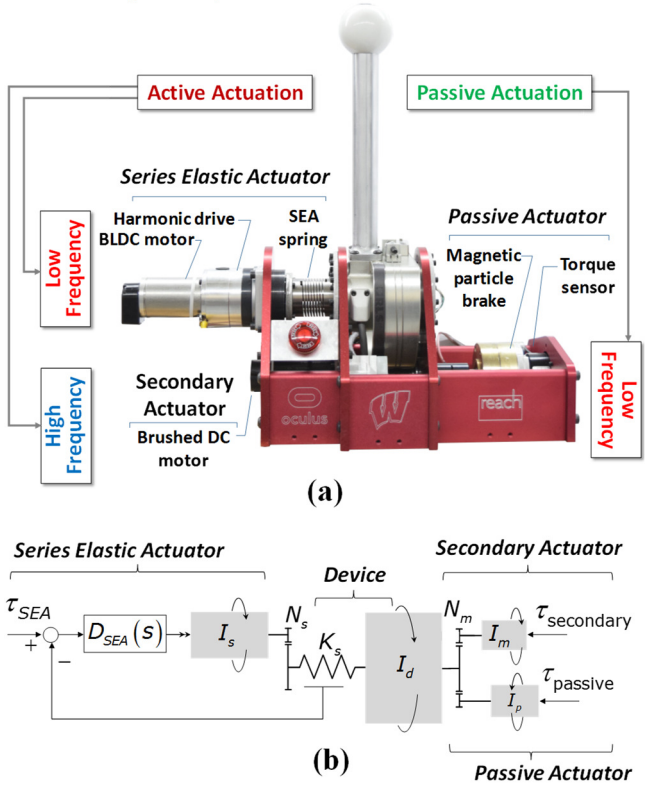

Figure 1. Overview of the Balanced Hybrid Active-Passive Actuation Approach. (a) one degree-of-freedom prototype; (b) lumped-parameter representation.

We discuss the design approach in more detail in the next section followed by a description of the control approach and the experimental validation of the new actuator.

III. Design Approach

The design effort focusses on achieving a high-performance haptics interface with a large torque bandwidth and low output impedance, to improve the rendering range and to maintain device transparency. The design also incorporates attributes that are required for the actuator torques to combine in parallel, with minimal mutual interference.

A. *Passive Actuator – Particle Brake*

Different passive actuation approaches, such as hysteresis brakes, MR and ER brakes, eddy current brakes and particle brakes, have been used in the past to build passive and hybrid haptic interfaces. Hysteresis brakes have a smooth operation and zero minimum friction but suffer from cogging torque. Eddy current brakes work well as active dampers but cannot produce torque at low or zero velocities. Researchers have used MR brakes, which have high torque densities but must be custom built as they are not commercially available is sizes appropriate for hand-held haptic interfaces. As an alternative, particle brakes have a relatively fast response time as compared to other passive actuators and have high torque density. In addition, they are commercially available in a wide range of sizes. They can provide static torque (at zero velocity) and have less nonlinear characteristics as compared to MR and hysteresis brakes. As such, a particle brake was selected as the passive actuator for the hybrid system described here. As part of the control approach (see Section IV), a torque sensor is incorporated into the drive train to provide direct measurement of the reaction torque from the brake. Finally, a low friction, low reduction cable transmission is used to increase the torque density of the passive actuator without significantly increasing its output impedance.

B. *Active Compliant Actuation - Series Elastic Actuator*

A series elastic actuator is incorporated to provide large low-frequency active torques while maintaining low output impedance. A series elastic actuator incorporates a spring in series with a large force and power actuator, usually accompanied by a high-reduction gearhead to amplify force or torque production. Using torque feedback, measured by sensing the spring deflection, the output impedance of the series elastic actuator can be significantly reduced, within the closed-loop bandwidth of torque controller, from that of the actuator and gearhead alone. Above the closed-loop bandwidth, the output impedance is determined by the spring stiffness. Thus, through proper tuning of the torque controller and proper selection of the spring stiffness, the series elastic actuator output impedance can be kept very low over a large frequency range, allowing for constructive summation of the various actuator output torques while providing high torque output. In general, the performance of a series elastic actuator improves with increasing closed-loop torque control bandwidth. As such, design elements that would limit the bandwidth, including gearhead backlash and spring deflection sensor noise should be minimized.

C. *Secondary Active Actuation – Small DC servomotor*

Large torque bandwidth is necessary for high-performance rendering capabilities. Both the series elastic actuator and the passive actuator have relatively slow response times, with typical time constants of 10 msec or larger. To recover the high-frequency content, a secondary actuator is added in parallel. The secondary actuator is selected with low inertia, fast response time and capable of high peak torque. A low friction, low reduction cable transmission is used to increase the torque density of the secondary actuator without significantly increasing its output impedance.

IV. Control Approach

In hybrid active-passive haptic interface implementations, researchers have explored different control paradigms to improve stability, rendering capabilities and minimize energy consumption [6, 7, 9, 10]. A common approach is to partition

the active and the passive torque components based on the calculated power [7, 9]. While intuitive, this approach can exacerbate the undesirable nonlinear behavior of the passive actuator that occurs during velocity reversals. Specifically, an active-passive partitioning approach can result in rapid switching between the active and passive actuator in situations that contain frequent velocity reversals concurrent with high rendering torque, as might occur when interacting with a stiff virtual wall. An example of this undesirable behavior is shown in Figure 2, where a one degree-of-freedom, hybrid haptic device prototype (described in subsequent sections of this paper) was controlled using a simple active-passive partitioning approach. The rapid switching results in excessive vibration with a notable loss of rendering quality. While low-pass filtering of the reference torque signal can reduce this effect, the phase lag introduced reduces the stabilizing effect of the passive actuator.

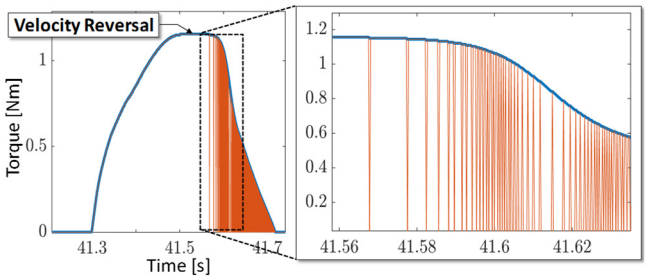

Figure 2. Time domain plot of the passive reference signals capturing the switching effects during velocity reversals while rendering a virtual wall.

A. *Cascaded Passive-Active Control Approach*

To avoid rapid switching between the active and passive actuation we have adopted an approach that continuously activates the passive actuator such that the switching torques are minimized. The advantage of this approach is seen in the improvements to the rendering quality, as the unwanted switching behavior is greatly reduced. The disadvantage of continuously activating the passive torque lies primarily in the need for larger active torques, in that passive torques must be cancelled during periods of active torque rendering. In implementations where the active and passive torques capabilities are not equal, a situation common to hybrid haptic actuation approaches other than the one described here, this control approach would be undesirable and likely infeasible in that the active torque capabilities of other approaches are commonly an order of magnitude less than the passive torque capabilities. However, in the balanced hybrid actuation approach described here, the active torque capability is equal to or greater than that of the passive actuation, primarily due to the large torque capability of the series elastic actuator.

The details of the control approach are shown in Figure 3. As shown in Figure 3, the desired rendering torque, τ^*_a, consisting of the complete torque command, active and passive torque included, is commanded to the passive actuator. The resulting passive actuator torque, measured using a torque sensor mounted on the passive actuator, is compared to the desired rendering torque to form the active torque command. Here, the slow dynamics of the passive actuator low-pass filters the reference command to the active actuator, significantly reducing the undesirable switching behavior. The active torque command is a summation of the active torque portion of the desired rendering torque, τ^*_a, the active torque required to counter-act the passive actuator's torque acting contrary to the desired active torque, and the passive actuator torque error.

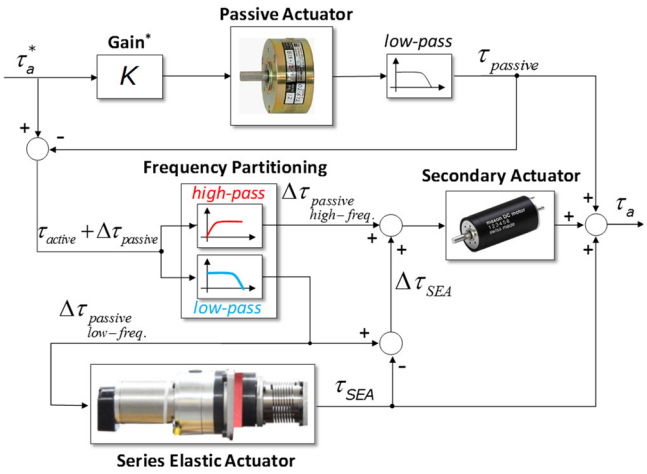

Figure 3. Block diagram representation of the Cascaded Passive-Active Only control approach. τ^*_a is the desired actuator torque and τ_a is the resulting actuator torque output from the three actuators. The gain* K is used to adjust the contribution of the passive actuator which is explained in detail in Section V. It is nominally set equal to 1.

The resulting active torque command is then frequency partitioned, where the low-frequency portion is commanded to the active series elastic actuator and the high-frequency portion is commanded to the small, fast secondary actuator. The frequency partitioning also helps in reducing the noise content from the measured brake torque signal which improves stability. Finally, the torque error term of the closed-loop series elastic actuator closed-loop controller is commanded to the secondary actuator.

The resulting control topology shown in Figure 3 results in a high-bandwidth rendered torque while significantly reducing the undesirable switching effect common to other hybrid implementations. In addition, the introduction of passive torque sensing, as part of the process in forming the active torque commands, results in greatly improved rendering accuracy. Errors in passive torque production, due to the highly nonlinear characteristics of the passive actuator, are typically large and result in unwanted effects at velocity reversals, commonly referred to as a sticky-effect. The measurement of the passive torque and the compensation of torque errors results in significantly improved torque rendering accuracy.

V. Experimental Validation

A one degree-of-freedom, high-performance, haptic device prototype was developed using the design approach described in Section III to evaluate the balanced hybrid active passive actuation approach. The design is optimized to reduce friction, compliance and other non-desirable effects that affect the performance and transparency of the device. The device was designed to provide a maximum force of 30 N and a maximum speed of 3 m/s.

To achieve the low-frequency active torque levels and a high bandwidth actuator, the series elastic actuator is designed using a low inertia 100 Watt Maxon brushless DC motor, a

zero backlash HD Systems harmonic drive with a 50:1 reduction and a machined spring from Helical. The actuator is instrumented with a linear output hall effect transducer (LOHET) analog sensor that measures magnetic flux. The relative deflection of the spring is measured by incorporating magnets into the spring assembly and measuring the change in flux through the LOHET as the magnets rotate. Figure 1 shows the design of the actuator.

A Placid Industries particle brake with a peak torque of 0.68 Nm was chosen for the passive actuation. As described in Section III, it is interfaced through a low friction cable drive mechanism with a reduction of 11:1. The cable reduction allows for the use of a smaller brake, thereby reducing the response time. The unpowered brake has residual friction of 0.023 Nm.

An ironless core 90 Watt Maxon brushed DC motor with low rotor inertia and no cogging torque was selected for the secondary active actuator. The fast response times and the peak torque capabilities (1.09 Nm) enable the secondary actuator to provide the high-frequency active torques. The selected motor is interfaced through the same low friction cable drive mechanism as the passive actuator.

The primary joint axis is instrumented with a high-resolution Renishaw Magnetic Linear Encoder used to measure the joint position and the user handle is instrumented with a 6-axis Force-Torque sensor (ATI Mini 27) to measure the output forces directly. The device is interfaced to a Speedgoat Real-Time Target controller. The control law is implemented using Simulink-Real Time (The Mathworks). The sample frequency is set at 3.5 KHz. Analog inputs, including the LOHET, brake torque sensor, and six-axis force/torque sensor, are filtered using a 2nd order Bessel filter with a cutoff frequency of 400 kHz. The electronics and harnesses are shielded to reduce the noise effects on the controller.

The experiments are designed to evaluate the hybrid actuation concept and the haptic performance of the device. The performance is compared to an active only system where the brake is disabled. The performance is evaluated by measuring the device's stable rendering range, tracking accuracy and transparency.

A. *Rendering Range*

One of the primary goals of the hybrid actuation approach is to improve the stable haptic rendering range. The initial set of experiments was designed to measure the maximum attainable virtual stiffness. The maximum stiffness is evaluated experimentally through a small user study. Specifically, users were instructed to grasp the device using their fingers and thumb, avoiding contact with their palm (see Figure 4), and to grasp with light pressure. The maximum stiffness was experimentally determined at the point which light, sustained oscillations are observed when the user taps against the virtual wall.

The virtual stiffness experiments were performed using the balanced hybrid active passive actuation prototype described earlier. To put the experimental results in context, the virtual stiffness experiments were also performed using a purely active device. In this case, the active device was realized by disabling the passive brake of the hybrid prototype. The active device is equivalent to the parallel actuation approach described in [14], which is a high performance impedance-based device with high forces and large power density.

The virtual stiffness experimental results for both the hybrid and active-only devices are listed in Table I. The measured force as a function of displacement for a representative trial is shown in Figure 5. The average maximum measured attainable stiffness for the hybrid active-passive approach and the active-only approach is approximately 159 N/mm and 48 N/mm, respectively.

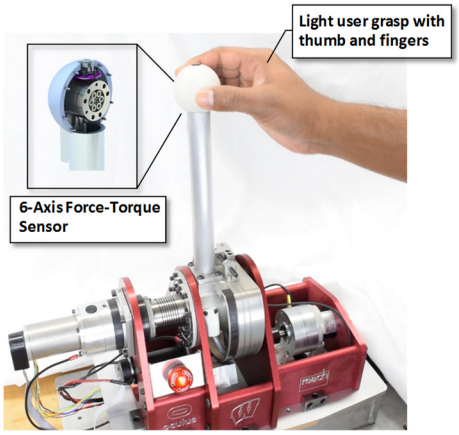

Figure 4. User holding the handle of the 1-DOF Hybrid Haptic Interface prototype with a light grasp, during a virtual wall interaction. The exploded view of the handle shows the embedded 6-axis Force-Torque sensor used for performance evaluation of the device.

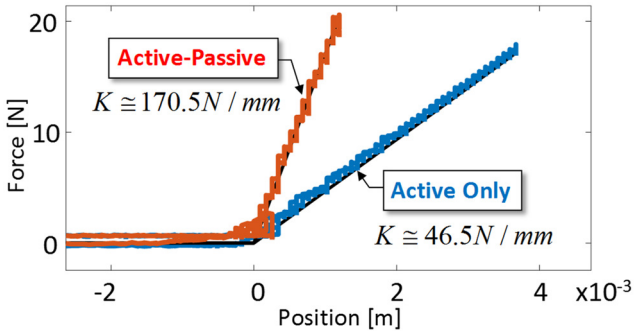

Figure 5. Plot comparing the achievable stiffness with the active only (blue) and the hybrid (red) approaches, for one of the user interactions with the virtual wall.

The active-passive actuation, controlled using the cascaded passive-active control approach describe in Section IV, has improved the stable rendering range by more than 300% as compared to the active only approach. The increased stable rendering range results from the increased energy dissipation that occurs due to the continuous brake activation.

TABLE I. RENDERING RANGE

	Stiffness	
	Active-Passive	*Active Only*
User 1	170.5 N/mm	46.5 N/mm
User 2	151.9 N/mm	44.9 N/mm
User 3	155 N/mm	54.2 N/mm

This can be understood by considering a scenario where the device begins to oscillate just prior to instability. Such a case would occur when interacting within a high stiffness virtual wall. For the hybrid case, motions that cause the device to move inward relative to the wall boundary are passive, resulting in a net dissipation of energy, while motions that cause the device to move outward may be active. For the active only case, both inward and outward motions are active. The additional passive energy dissipation of the hybrid device result in higher achievable virtual stiffness rendering.

B. *Accuracy – Large Stiffness*

The second set of experiments were performed to assess the rendering accuracy, a measure of how well the actuator torque tracks the desired torque. For this experiment, users were asked to tap or press into the virtual wall using a variety of grasps. The measured torque and the desired torque, as dictated by the specified virtual stiffness, was recorded. The rendering accuracy was assessed by calculating the maximum deviation between the desired and measured torque. The virtual stiffness levels used in the evaluation were equal to approximately 50% of the maximum attainable virtual stiffness for each approach.

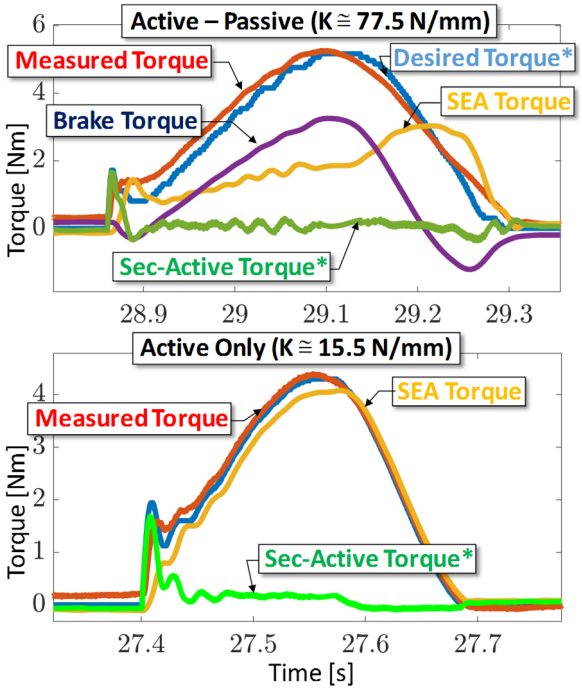

Figure 6. Time domain plot of the joint and the actuator torques while rendering a stiff virtual wall using the active-passive approach (left) and the active only approach (right).

Figure 6 shows the time domain plots of the joint and the actuator torques for the active-passive (left) and the active only (right) approaches for an example user interaction with a virtual wall. The blue signal corresponds to the desired joint torque corresponding to a rendered stiffness of 77.5 N/mm for the active-passive approach and 15.5 N/mm for the active only approach. The measured joint torque, calculated from the force-torque sensor mounted on the handle, is shown in red. We see from Figure 6 that the rendered accuracy is good for both the hybrid and active-only approach, with a maximum deviation between the measured and desired torque of less than 0.5 N, and, more importantly, that the rendering accuracy of the hybrid approach is comparable to that of the active only case.

Unlike many hybrid actuation implementations, the control approach described here directly measures the passive brake torque signal which is used in turn to calculate the active actuator torque command, the summation of which results in a close match to the desired torque. This control approach is advantageous in that errant brake torques, such as those that occur due to brake velocity reversals or residual brake torque during free-space motion, are largely cancelled by active actuation, including the series elastic actuator and the fast, secondary actuator.

C. *Accuracy – Low Stiffness*

To assess the rendering accuracy for low stiffness rendering, a similar experiment was conducted for virtual stiffness levels significantly less than the maximum attainable stiffness. Figure 7 shows the time domain plots of the joint and the actuator torques for the active-passive (left) and the active only (right) approaches for an example user interaction with a virtual wall of stiffness 1.5 N/mm.

We see from Figure 7 that the rendered accuracy of the hybrid approach is poor as compared to the active-only approach. For the hybrid active-passive approach, we observe a pronounced deviation between the desired and actual torque that occurs during the velocity reversal (at peak wall penetration). The large residual brake torque (relative to the desired torque) is not effectively canceled by the active actuation, resulting in poor rendering accuracy.

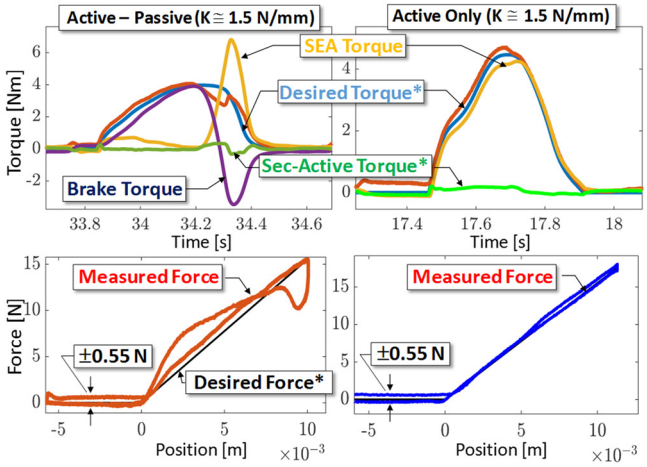

Figure 7. Time domain (top) and stiffness plot (bottom) comparing the rendering accuracy of the active-passive (left) and the active only (right) approaches

D. *Modified Control Approach*

To recover the rendering accuracy while also maintaining the high rendering range we can modify control approach presented in Section IV. The control approach described in Section IV is modified to include a gain term applied to the passive command. The gain K, shown in the block diagram in Figure 3, modulates the contribution of the passive actuator such that when K is set equal to 1.0, the control structure is as described in Section IV and when K is set equal to 0.0, the

control structure is equivalent to the parallel actuation approach described in [14].

In practice, the control algorithm can be adjusted based on the stiffness of the current rendered surface, detectable in real-time by evaluating the ratio of desired force to normal surface penetration. The simplest approach would be to define a stiffness threshold above which the hybrid controller would be used and below which the parallel active actuator controller would be used. An example of this approach is shown in Figure 8, where the stiffness threshold was chosen as 38 N/mm.

Figure 8 shows time domain and stiffness plots from two virtual wall interactions with varying stiffness. The control approach is set to the active-passive approach by default. It can be observed that it toggles to active only approach in the first interaction and toggles back to active-passive in the second high stiffness interaction. The time domain and stiffness plots for the two interactions are shown and we see that these are stable interactions with good rendering accuracy.

E. Device Transparency

The experiments described in the previous section can be used to assess device transparency, defined here as the residual force displayed during free-space motion. For both the hybrid active-passive device and the parallel active actuation approach, the residual forces were ±0.55N (see Figure 7). The measured residual forces are attributable to the device friction associated with the joint bearings and the cable-reduction. These results demonstrate that the hybrid active-passive approach is effective in compensating for the residual friction from the unpowered passive actuator, resulting in the same level of transparency as the active only approach.

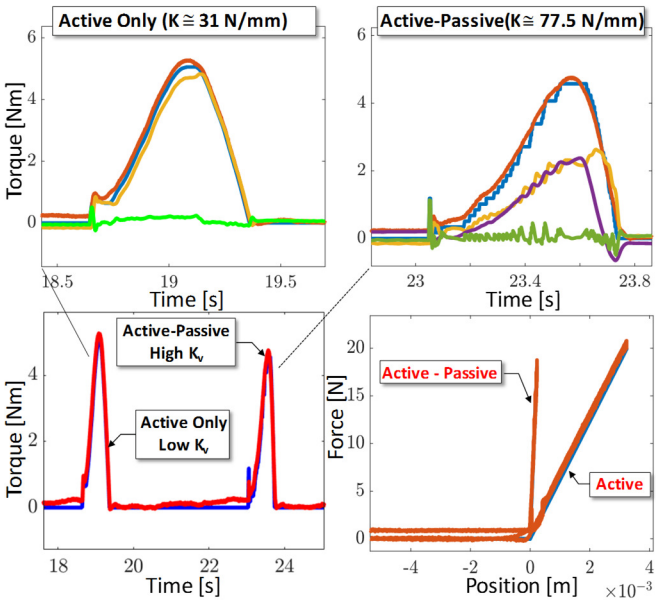

Figure 8. Time domain and stiffness plots of the modified control approach, showing good rendering accuracy for both low and high rendered virtual stiffness K_v, as the controller toggles between the active only and active-passive approaches respectively.

VI. Summary

A new balanced hybrid actuation approach for high-performance haptic interfaces has been described along with a candidate control approach. The approach addresses the active-passive torque asymmetry common to hybrid actuation by combining a high-power, low-impedance active compliant actuation (series-elastic actuator) with energy absorbing high-force passive actuation in parallel with a fast, low-power secondary active actuation. The approach was validated with a one degree-of-freedom prototype and experimental results show the improved rendering range compared to an active only approach. The transparency and tracking accuracy were also compared to demonstrate the performance of the device. A modified control approach was presented to improve the tracking accuracy at lower stiffness.

Acknowledgements

This research work was made possible by funding from Facebook Reality Labs.

References

[1] N. Diolaiti, G. Niemeyer, F. Barbagli, and J. K. Salisbury, "Stability of Haptic Rendering: Discretization, Quantization, Time Delay, and Coulomb Effects," Robotics, IEEE Transactions on, vol. 22, no. 2, pp. 256-268, 2006.

[2] J. J. Abbott and A. M. Okamura, "Effects of position quantization and sampling rate on virtual-wall passivity," IEEE Transactions on Robotics, vol. 21, no. 5, pp. 952-964, 2005.

[3] N. Colonnese and A. Okamura, "Stability and quantization-error analysis of haptic rendering of virtual stiffness and damping," The International Journal of Robotics Research, vol. 35, no. 9, pp. 1103-1120, August 1, 2016 2016.

[4] C. Parthiban and M. Zinn, "Performance and Stability Limitations of Admittance-based Haptic Interfaces," presented at the IEEE Haptics Symposium, San Francisco, March 25-28, 2018, 2018.

[5] J. E. Colgate and J. M. Brown, "Factors affecting the Z-Width of a haptic display," in Robotics and Automation, 1994. Proceedings., 1994 IEEE International Conference on, 1994, pp. 3205-3210 vol.4.

[6] J. An and D.-S. Kwon, "Stability and Performance of Haptic Interfaces with Active/Passive Actuators—Theory and Experiments," vol. 25, no. 11, pp. 1121-1136, 2006.

[7] C. Rossa, J. Lozada, and A. Micaelli, "Design and Control of a Dual Unidirectional Brake Hybrid Actuation System for Haptic Devices," IEEE Transactions on Haptics, vol. 7, no. 4, pp. 442-453, 2014.

[8] A. Jinung and K. Dong-soo, "Haptic experimentation on a hybrid active/passive force feedback device," in Proceedings 2002 IEEE International Conference on Robotics and Automation (Cat. No.02CH37292), 2002, vol. 4, pp. 4217-4222 vol.4.

[9] A. Jinung and K. Dong-Soo, "Control of multiple DOF hybrid haptic interface with active/passive actuators," in 2005 IEEE/RSJ International Conference on Intelligent Robots and Systems, 2005, pp. 2572-2577.

[10] C. François and K. Oussama, "A New Actuation Approach for Haptic Interface Design," The International Journal of Robotics Research, vol. 28, no. 6, pp. 834-848, 2009/06/01 2009.

[11] A. H. C. Gosline and V. Hayward, "Eddy Current Brakes for Haptic Interfaces: Design, Identification, and Control," IEEE/ASME Transactions on Mechatronics, vol. 13, no. 6, pp. 669-677, 2008.

[12] M. Antolini, O. Köse, and H. Gurocak, "A first order transfer function to balance the workload in brake-motor hybrid actuators," in 2014 IEEE Haptics Symposium (HAPTICS), 2014, pp. 509-514.

[13] A. Jinung and K. Dong-Soo, "In haptics, the influence of the controllable physical damping on stability and performance," in 2004 IEEE/RSJ International Conference on Intelligent Robots and Systems (IROS) (IEEE Cat. No.04CH37566), 2004, vol. 2, pp. 1204-1209 vol.2.

[14] M. Zinn, O. Khatib, B. Roth, and J. K. Salisbury, "Large Workspace Haptic Devices - A New Actuation Approach," in Haptic interfaces for virtual environment and teleoperator systems, 2008. haptics 2008. symposium on, 2008, pp. 185-192.